MINIATURIZED AUTONOMOUS DISTRIBUTED SPACE SYSTEM FOR FUTURE SCIENCE AND EXPLORATION

Simone D'Amico,[*] Marco Pavone,[†] Shailendhar Saraf,[‡] Abdulaziz Alhussien,[§] Turki Al-Saud,[**] Sasha Buchman,[††] Robert Byer,[‡‡] Charbel Farhat,[§§]

Two key trends have the potential to revolutionize the way humans conduct space-flight, namely, the miniaturization of satellites (e.g., micro- and nano-satellites) and the distribution of payload tasks among multiple coordinated units (e.g., spacecraft formation-flying, on-orbit servicing/robotics, fractionation, swarms). The combination of these approaches is leading to a new generation of space architectures, so-called distributed space systems, which promise breakthroughs in space science, planetary science, and exploration. Based on the experience gained from the most recent flight demonstrations of autonomous spacecraft rendezvous and formation-flying (e.g., PRISMA, TanDEM-X), this paper describes a first-of-a-kind space technology and science program under implementation by the KACST-Stanford's Center for Excellence in Aeronautics and Astronautics in collaboration with national and international partners in the time frame of 10 years. The ultimate goals are to 1) develop a multi-purpose reconfigurable precise distributed space system based on microsatellite platforms, and 2) demonstrate its unprecedented capabilities in areas such as earth gravimetry and system dynamics, gravitational waves detection, and on-orbit servicing.

MOTIVATION: APPLICATIONS OF A DISTRIBUTED SPACE SYSTEM

In the most general sense, a Distributed Space System (DSS) involves two or more spacecraft which interact to accomplish a mission objective[1-2]. The concept is not new, and the first formation flying and rendezvous experiments were conducted in the 1960s and 1970s by the Soviet Union

[*] Assistant Professor, Department of Aeronautics and Astronautics, Stanford University, Stanford, CA 94305, e-mail: damicos@stanford.edu.
[†] Assistant Professor, Department of Aeronautics and Astronautics, Stanford University, Stanford, CA 94305, e-mail: pavone@stanford.edu.
[‡] Research Engineer, Hansen Experimental Physics Laboratory, Stanford University, 452 Lomita Mall, Stanford, CA 94305, e-mail: saraf@stanford.edu
[§] Co-Director, Center for Excellence in Aeronautics and Astronautics, King Abdulaziz City for Science and Technology (KACST), P.O Box 6086, Riyadh 11442 Saudi Arabia, e-mail: ahussien@kacst.edu.sa.
[**] President, King Abdulaziz City for Science and Technology (KACST), P.O Box 6086, Riyadh 11442 Saudi Arabia, e-mail: tal-saud@kacst.edu.sa.
[††] Professor, Hansen Experimental Physics Laboratory, Stanford University, 452 Lomita Mall, Stanford, CA 94305, e-mail: sbuchman@stanford.edu
[‡‡] Professor, Hansen Experimental Physics Laboratory, Stanford University, 452 Lomita Mall, Stanford, CA 94305, e-mail: rlbyer@stanford.edu
[§§] Chair, Department of Aeronautics and Astronautics, Stanford University, Stanford, CA 94305, e-mail: cfarhat@stanford.edu.

and the US[3]. However, historic missions had very short duration, little to no cost constraints, and were supported by extensive ground control. Contemporary missions of distributed space systems can be considered to start with the autonomous formation flying of the Japanese ETS-7 in 1998[4], followed by on-orbit-servicing technology demonstrations such as AFRL's XSS-11 (2005)[5] and DARPA's Orbital Express (2007)[6]. The most recent and advanced accomplishments in this area are represented by the Swedish PRISMA[7] and the German TanDEM-X[8] missions, both launched in 2010. In contrast to historic missions, these systems are characterized by long mission durations, autonomous relative navigation and control, and tight cost constraints. Despite a cost reduction of about one order of magnitude per spacecraft (from $1,000M to $100M dollars), these platforms are still prohibitively expensive. They are characterized by long development cycles and high risk due to the lack of redundancy (each satellite is a single point of failure). In addition the adoption of only two spacecraft limits the sensitivity of the synthetic aperture to the inter-spacecraft line-of-sight direction. This research and development program aims at overcoming the identified limitations of current distributed space systems by leveraging the recent tremendous progress of microsatellites (i.e., 10-100 kg wet mass), which are becoming a standard platform for scientific instrumentation.

The potential applications of DSS can be divided in three broad areas, namely planetary science, space science, and exploration and could impact multi-billion-dollar markets in earth remote sensing, disaster prediction and monitoring, and on-orbit servicing (see Fig. 1). In the planetary science domain, multiple closely flying satellites can be used to build instruments such as synthetic aperture radar interferometers (e.g., TanDEM-X) or gradiometers (e.g., GRACE, GRAIL) for spaceborne remote sensing and surveillance[9]. In particular radar data obtained from separated antennas which illuminate simultaneously a given target can be differenced to obtain accurate measurements of terrain height (e.g., cross-track interferometry for digital elevation modeling) or the velocity of on-ground objects such as cars or ships (e.g., along-track interferometry for traffic monitoring). Similarly closely flying accelerometers or drag-free satellites can be used to reconstruct the earth's gravity field (static and dynamics) to unprecedented levels of resolution. Precision inter-satellite tracking can provide simultaneous measurements in several spatial directions to estimate the full gravity gradient tensor. This might prove essential to isolate independent gravity field components and help resolve numerous physical processes which are not observable today through current spaceborne gravimeters (e.g., bathymetry and tectonics, hydrology, silent earthquakes, post-seismic deformations)[10]. DSS can potentially discover and monitor oil reservoir or ground water variations and resource depletion by rapid measurements of gravitational anomalies using multiple drag-free satellites.

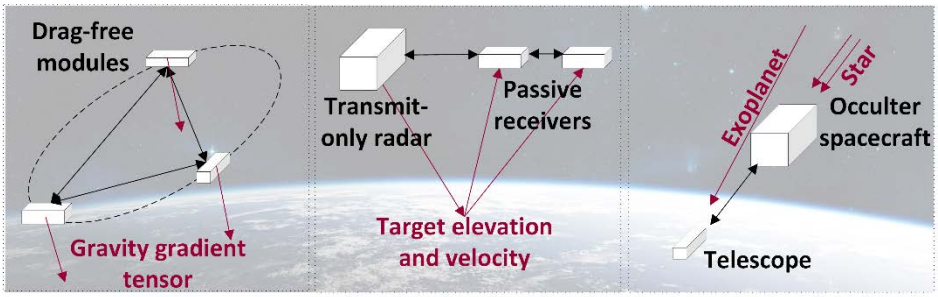

Figure 1. Example Conceptual Distributed Space Architectures. Left: Post-GRACE gradiometry. Middle: Post-TanDEM-X synthetic aperture radar interferometry. Right: Post-KEPLER exoplanet finder.

In the space science domain, dual-spacecraft telescopes can be used to conduct detailed spectral investigation of astronomical sources (e.g., XEUS, SIMBOL-X)[11], and to directly image terrestrial exoplanets (e.g., NWO)[12], while multi-spacecraft interferometers in the infrared and visible wavelength regions are considered as a key to new astrophysics discoveries such as in gravitational

physics (e.g., LISA, LAGRANGE)[13]. At its most precise performance level, a DSS of three or more spacecraft can form a gravitational wave observatory capable of detecting massive black hole binaries, or even a synthetic aperture optical telescope with greatly enhanced resolution over single satellite-based instruments.

In the space exploration and situational awareness domain, DSS technology can be used in a cooperative or non-cooperative fashion to assemble larger structures in space, inspect and characterize near-earth objects, and conduct on-orbit servicing tasks such as satellite repair, refueling, and disposal. In the longer term, novel DSS architectures such as swarms and fractionated spacecraft will establish powerful networks in space with exceptional characteristics (e.g., System F6)[14]. The aforementioned mission concepts are characterized by different levels of complexity, mainly dictated by the payload metrology and actuation needs, and typically require a high level of on-board autonomy to satisfy the requirements posed on relative navigation and control accuracy. This demand indicates clearly the necessity of precursor technology demonstration missions.

To this end, we propose a first-of-a-kind space technology and science program to be implemented at the KACST-Stanford's Center for Excellence in Aeronautics and Astronautics in collaboration with national and international partners in the time frame of 10 years. The ultimate goals are to 1) develop a multi-purpose reconfigurable precise distributed space system based on microsatellite platforms, and 2) demonstrate its unprecedented capabilities in areas such as earth gravimetry and system dynamics, gravitational waves detection, and on-orbit servicing.

TECHNOLOGY AND SCIENCE DEVELOPMENT ROADMAP

Tremendous challenges at system and subsystem level are faced when implementing DSS. In particular seven key research areas are identified as enabling technologies by the proposed program as illustrated in Fig. 2. These cover all relevant aspects from guidance, navigation, and control (Fig. 2, column 1-3), to drag-free, accelerometer technology, timekeeping, and communication (Fig. 2, column 4-6), all the way to mission design, planning, and exploitation (Fig. 2, column 7).

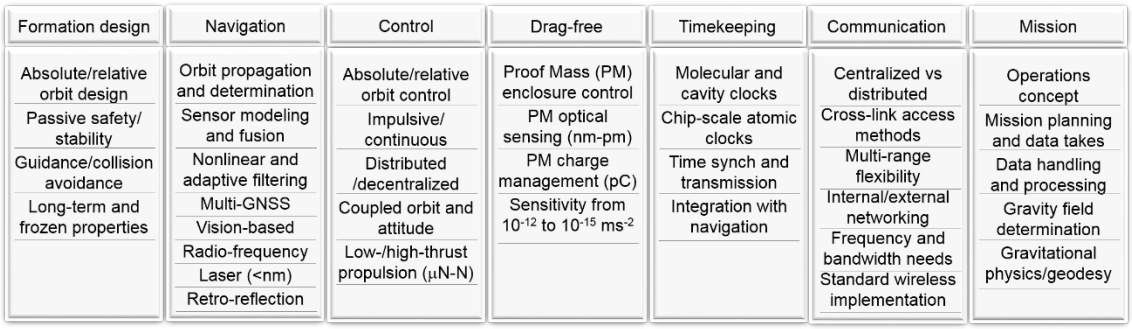

Figure 2. Technology Breakdown. Technologies proposed for development in this program.

Irrespective of the specific application, future DSS require an unprecedented level of autonomy to maintain and reconfigure the relative motion of the participating vehicles within the prescribed accuracy. Multi-stage distributed metrology systems are required capable of providing coarse (e.g., km/m level) to precise (e.g., cm/mm level) and ultra-precise (e.g., nm level) relative navigation under a variety of formation flying geometries, ranges, and operational scenarios (e.g., safe modes vs. routing operations). The stages of such a high dynamics range navigation system will be dependent from one another and possibly be fused. The proposed technology program aims at the fusion and seamless transition between multi-constellation Global Navigation Satellite System (GNSS), vision-based (optical and infrared), radio-frequency (based on pseudolites), and laser navigation. The initialization of each subsequent stage of the navigation system will be based on coarse

measurements from the previous stage and ultimately on ground-based orbit determination. The navigation system feeds a versatile formation guidance and control module. Depending on the formation flying scenario, both quasi-continuous forced motion and sparse impulsive maneuvering will be required. In many cases a hybridization of continuous and discrete control schemes will be necessary to satisfy the science payload requirements and the geometry constraints (e.g., from metrology or collision avoidance) simultaneously. Advanced DSS for surveillance and rapid response will require simultaneous precision control of absolute and relative orbit motion. Overall these requirements demand multiple propulsion systems capable of delivering low thrust (micro- to milli-Newton) and high thrust (sub-Newton). Nearly identical needs arise from trajectory control for autonomous rendezvous and docking, where passive relative orbits are used for far-range and initial approach operations, whereas forced motion control is required for close-in inspection and contact operations. Similar to the aforementioned navigation tasks, no absolute/relative low-/high-thrust control systems are available today to fulfil these requirements.

Among all applications of DSS, a special and unique role in the proposed technology development program is played by gravitational physics, both fundamental and for geodesy. The necessary drag-free technologies (Fig. 2, column 4) aims at a gravitational reference sensor with three translational degrees of freedom with residual acceleration noise below 10^{-12} m/s^2 for geodesy and 10^{-15} m/s^2 for gravitational waves detection. This is complemented by timekeeping and synchronization capabilities beyond state-of-the-art (Fig. 2, column 5). Proposed space capable clock systems include molecular iodine clocks, optical cavity resonators, and the most recent commercially available chip-scale atomic clocks.

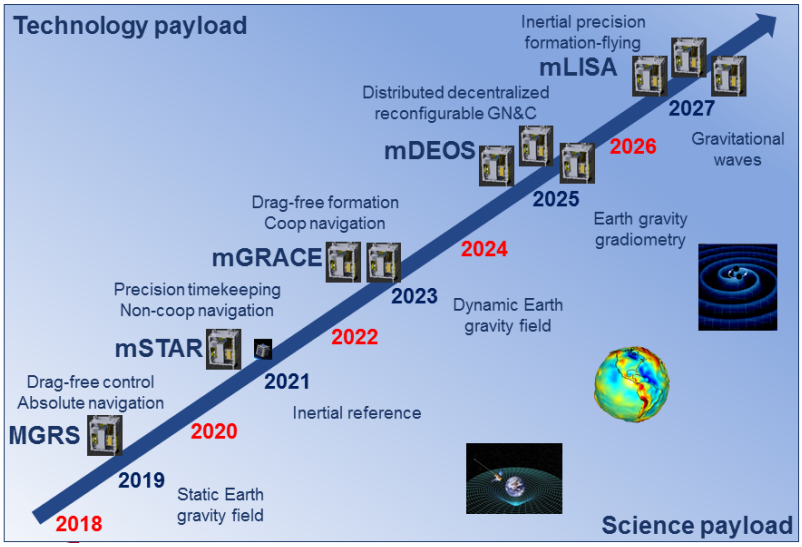

Figure 3. Roadmap milestones. Ground-based high-fidelity laboratory demos (red time tags), and space-based mission demos (blue time tags) leading to a miniaturized autonomous DSS for future science and exploration.

The proposed multi-purpose reconfigurable precise DSS is based on the SaudiSat microsatellite platforms[15]. An overview of the research and development roadmap is illustrated in Fig. 3. In particular the technology (Fig. 3, upper left area) and science (Fig. 3, bottom right area) objectives described in the previous sections are fulfilled within a timeframe of about 12 years (2015 – 2027). According to space system engineering practice, this is done in a stepwise monotonic approach where multiple technologies are brought from low to high technology readiness level (TRL 3 to 9). Each technology is first developed and demonstrated in a ground-based high-fidelity laboratory

environment at Stanford University (Fig. 3, red time tags) and later deployed for flight demonstration on-orbit (Fig. 3, blue time tags). A total of five missions are proposed for development and execution every other year, namely the Modular Gravitational Reference Sensor (MGRS) in 2019, the Miniaturized Space Time Asymmetry Research on a Small Satellite (mSTAR) in 2021, the Miniaturized Gravity Recovery and Climate Experiment (mGRACE) in 2023, the Miniaturized Distributed Earth Orbiting System (mDEOS) in 2025, and the Miniaturized Laser Interferometer Space Antenna (mLISA) in 2027. Each mission provides lessons learned and is succeeded by laboratory demonstrations one year after. In addition each mission is conceived to act as backup of the previous mission in case of a major failure.

THE FIRST MILESTONES: MGRS AND MSTAR

The first two missions of the proposed program are intended to kick-off the development of most of the technologies identified in Fig. 2. They are planned for launch in Low Earth Orbit (LEO) with near-polar inclinations and near-frozen eccentricity to maximize the science throughput. They employ the same SaudiSat bus which is under development at the KACST in Saudi Arabia. It targets a wet mass of 100 kg, an envelope size of 650x600x1200 mm, and power generation up to 100 W. SaudiSat will support three-axis attitude determination based on sun-sensors, magnetometers, and star-trackers, three-axis attitude control based on magnetorquers and cold-gas propulsion, data downlink rate at 358 Mb/s, data storage of 28 Gbytes at speed rate of 25 MB/s and compliance with the Russian Dnepr and Indian Polar Satellite Launch Vehicle (PSLV) launch vehicles. The MGRS and mSTAR mission operations are designed to use existing resources among partner institutions wherever possible. The mission control center will be located at KACST in Riyadh. KACST will lead mission operations by providing communications link scheduling, activity planning and command sequencing, command product verification, activity execution (commanding/telemetry monitoring), and supplementary space vehicle and instrument engineering assessment (space vehicle performance estimation, link assessment, etc.). Emergency resources will be available through the NASA Earth Ground Network. All science and spacecraft bus data will be passed to the partners for evaluation and processing.

Each mission is motivated by concise technology and science statements which are described below. MGRS is currently planned for 2019 and will demonstrate drag-free technologies with aimed residual acceleration noise below 10^{-12} m/s^2. This requires micro- to milli-Newton quasi continuous actuation in combination with precision laser tracking of the inner proof mass at nanometer accuracies (3D). The primary science objective of MGRS is the determination of the static earth gravity field with improvement of up to two orders of magnitude in accuracy as compared with ground-based observations. This will be possible thanks to the dedicated orbit design, continuous multi-GNSS satellite-to-satellite tracking capability (cm-level orbit determination accuracy) together with indirect measurement of the non-gravitational orbit perturbations. Although the expected accuracy can be compared with the results of the recently flown German CHAMP mission, MGRS will be realized at a tiny fraction of the cost and will pave the way for the subsequent missions of this roadmap.

Lessons learned from MGRS and dedicated laboratory demonstrations will precede the launch of mSTAR in 2021. This collaborative mission has two fundamental technology objectives, namely 1) the demonstration of unprecedented timekeeping capabilities using molecular iodine clocks, and optical cavity resonators, and 2) the demonstration of vision-based far- to mid-range rendezvous relative to a non-cooperative CubeSat carried and ejected on-orbit by the mother spacecraft. The latter objective requires the adoption of a dedicated optical camera for angles-only navigation and the usage of a high-thrust (sub-Netwon) propulsion system for impulsive control. The science objective of mSTAR is an advanced Kennedy-Thorndike (KT) test of special relativity using the large

and rapid velocity modulation available in LEO. An improvement of about two order of magnitudes over present ground results are expected. The KT experiment searches for boost dependent Lorentz invariance violations which might revolutionize physics if found.

The successful execution of advanced missions such as MGRS and mSTAR will mature the fundamental navigation, control, timekeeping, and drag-free technologies needed to realize a multi-purpose DSS. At the same time, breakthroughs in gravitational physics and on-orbit servicing will push the boundaries of space science and exploration. The next sections describe the key payload technologies and the related challenges for MGRS and mSTAR in more details.

THE MGRS MISSION: KEY PAYLOAD TECHNOLOGIES

Science Payload

After the first generation of dedicated satellite missions for the precise mapping of the earth's gravity field and the recovery of the related geophysical processes (CHAMP, GRACE, and GOCE)[10], earth scientists consider three possible ways to improve the state-of-the-art: 1) achieving a higher precision to improve the quantification of phenomena already measured by GRACE and GOCE, 2) increasing the spatial and temporal resolution to resolve numerous geophysical processes which are difficult to resolve today (e.g., coastal currents, bathymetry, ice bottom topography, hydrology, deep ocean studies), 3) improving precision and resolution simultaneously to separate and isolate individual effects. Next generation gravity missions can be enabled by drag-free DSS technology thanks to the simultaneous inter-satellite tracking in several spatial directions. As a first milestone, MGRS intends to achieve the first objective described above by making more precise estimates of the low-order coefficients in the spherical harmonic representation of the geopotential (below order and degree 20). In particular, Fig. 4 (left) shows the target gravity anomaly error of MGRS ($<10^{-3}$ mGal for degree < 20) as compared with the current estimates from the GRACE and GOCE missions[16].

In order to achieve this objective, two key requirements are posed on the MGRS orbit. First, the target orbit must be as low and as repeatable as possible in the earth-centered earth-fixed frame so that small changes in the gravity field between repeat cycles can be separated out. Second, the actual MGRS orbit, or more specifically the orbit of its proof mass, must be reconstructed post-facto with an accuracy of 1 cm (3D, standard deviation). Dedicated algorithms and software facilities are under development at Stanford to 1) generate an MGRS orbit which maximizes the science throughput, and 2) enable precise reduced-dynamics orbit and gravity determination based on spaceborne Global Navigation Satellite System (GNSS) technology.

The orbit design process is schematically illustrated in Fig. 4 (right) and is inspired by the methods used in the TerraSAR-X mission[17]. An initial guess is based on the secular earth's oblateness J_2 effects which are known in closed form. An iterative process is then defined which refines the initial osculating orbit elements to obtain an exact repeat cycle of 30 days with 477 orbits (seasonal temporal resolution), a sun-synchronous dawn-dusk orbit (steady power and thermal environment), and a frozen orbit with constant eccentricity vector (no altitude variations). The orbit is numerically integrated using a high-accuracy numerical propagator which accounts for conservative forces only, namely 120x120 GRACE's static gravity field, sun and moon third-body, and relativistic effects. In addition, state-of-the-art conversion between the earth-centered-inertial (J2000) and the earth-centered earth-fixed (WGS84) reference frame are adopted.

As a baseline, the GNSS-based precise orbit determination strategy assumes a nominal drag-free control performance and estimates the proof mass orbit in conjunction with the desired coefficients of the geopotential. All un-modelled perturbations are captured by second-order Gauss Mar-

kov processes in the form of empirical accelerations in the radial, along-track, and cross-track directions[18]. These can be used to evaluate the behavior of the drag-free control system and even aid its performance during mission operations. Upon necessity, high-fidelity models of the propulsion system and all forces acting on the MGRS proof mass can be included in the orbit determination process, such as magnetic interaction, cosmic ray impacts, optical sensing, thermal effects, Brownian effects, self-gravity, and electric disturbances. The baseline GNSS hardware system consists of a commercial-off-the-shelf dual-frequency receiver (current candidates are the Javad Triumph DG3TH and the NovAtel OEM4-G2L) and a choke ring antenna to minimize multi-path effects[19].

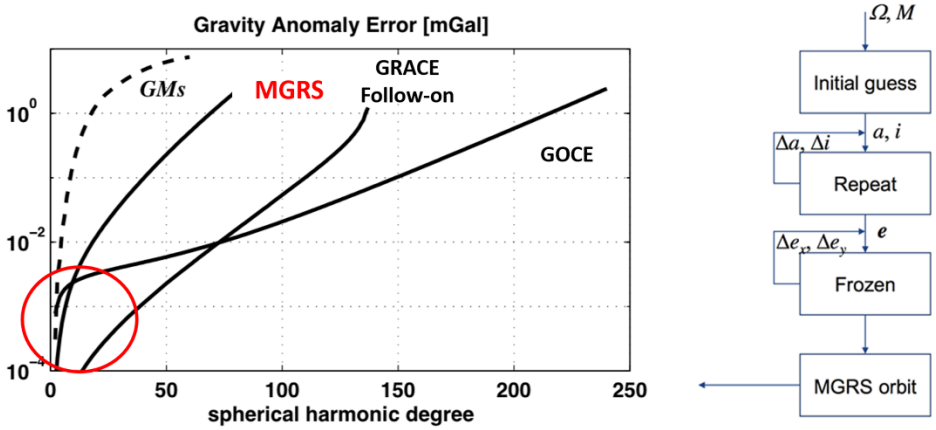

Figure 4. MGRS science and orbit. MGRS aims at improving precision of the gravity field recovery by estimating low order and degree coefficients of the geopotential (left). To this end, the target orbit of MGRS is optimized to ensure the highest repeatability in the earth-centered earth-fixed reference frame (right).

Technology Demonstration Payload: Drag-Free Sensor

The key sensor of MGRS is an ultra-quiet spherical inertial reference that operates in a drag-free environment aboard the satellite. Spherical inertial sensors have a long history dating back to the early '70s. The first drag-free satellite, TRIAD I with the DISturbance COmpensation System (DISCOS), was launched in 1972 and achieved a drag-free performance of less than 10^{-10} m·s^{-2} over two weeks, limited by orbit determination accuracy (pre-GPS)[20]. Since then, two more drag-free satellites have been flown: NASA's relativity mission, Gravity Probe B (GP-B)[21] and ESA's geodesy mission, GOCE[22]. TRIAD I and GP-B were drag-free in all degrees of freedom while GOCE was drag-free in one translational degree of freedom only. The results from the GP-B mission demonstrated the importance of patch effects on the drag-free performance and in particular showed the need for housing gaps of the order of the test mass (TM) dimensions[23].

The drag-free sensor utilizing a spherical TM, as in GP-B and DISCOS, has been under development at Stanford for a wide range of applications since 2004[24]. The primary components of the sensor include a spherical TM of 2.5 cm in diameter, inside a housing where the gap to the walls equals the ball radius. The TM location in the housing is determined to nanometer accuracy by an eight-beam differential optical shadow sensor (DOSS)[25]. The principal advantages of this design compared to previous drag-free configurations are: 1) no active forces applied to the TM; 2) large gaps to the housing reduce patch effect forces dramatically[23]; 3) simplicity and reliability; 4) minimization of ancillary electronics and control loops; and 4) long flight heritage of the core technology[20-21]. The caging (launch-lock) mechanism and the charge control system are based on the GP-B design with improvements from modern light emitting diodes (LED) as ultraviolet (UV) sources[26].

The laboratory model for the TM drag-free system is completed and the functionality of a caging system has been successfully verified in parabolic zero-gravity plane flights[27]. The material for the TM needs to meet a number of requirements. It needs to allow easy fabrication of a very round sphere and be compatible with the low disturbances required by the instrument. In particular, it needs to be of high density to minimize the acceleration due to surface forces, and of low magnetic susceptibility and out-gassing. The baseline choice is a low iron impurity BeCu alloy UNS C17000 (8,820 kg·m^{-3}), that has been verified for low magnetic susceptibility[28-29]. An alternative is AuPt (19,440 kg·m^{-3}) as used in DISCOS, but this material undergoes spinodal decomposition when cast, making it more difficult to work with.

The functionality of the nm read-out system will be verified in space, with laboratory tests already ensuring a high level of confidence in its performance. DOSS measures the position of the TM relative to the housing. A complete system has been developed and tested at Stanford, using flight-like components and circuits. The optics system has achieved a measured sensitivity below 10 nm·Hz$^{-1/2}$ above 10 mHz, with a trend inversely proportional to frequencies below 10 mHz. DOSS is based on measuring light intensity and allows for a large dynamic range which is only limited by the size of the detector and the beam waist. Two light beams of equal intensity are tangent to and partially blocked by the TM. The two intensities and their difference are measured, thus canceling common mode noise signals. The measurement principle is illustrated in Fig. 5 for a 2-dimensional measurement with 2 pairs of detectors that cancel radiation pressure.

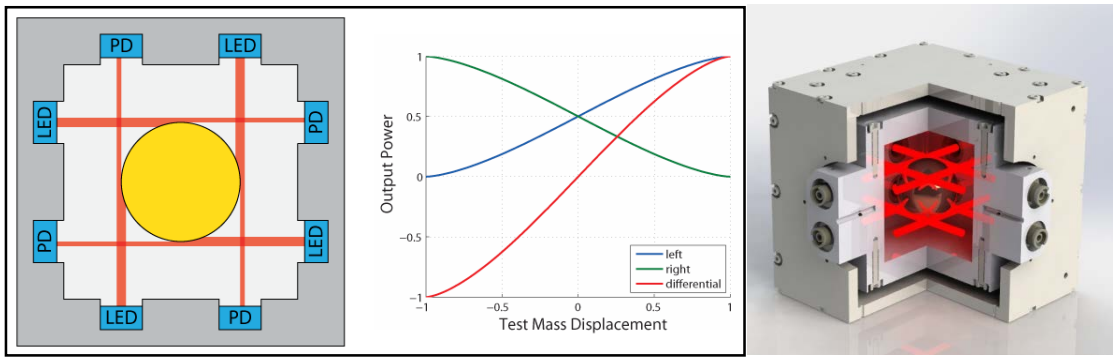

Figure 5. Drag-free sensor. Shadow sensor concept with TM, four detectors and partially blocked light beams (left). Simulation of the left and right signals and their difference for one axis (middle). Cutout of the 2-layer thermal enclosure showing the TM and simulated light beams (right).

Charge management of the TM is accomplished by UV photo-emission using commercially available LED operating in the 240-255 nm range[26] as the UV source. A number of UV-LED devices have successfully completed environmental testing, and a complete charge control system using UV LED has been flown on a SaudiSat in 2014[30]. This mission has verified the ability to perform charge management in space using long-lifetime, low-power LED emitting at 255nm. Compared to Hg lamps, UV LED are smaller and lighter, consume less power, have a wider spectrum selection, and a much higher dynamic range, with at least an order of magnitude improvement in each performance area. The power output is also very stable, with a lifetime of more than 30,000 hours. By using UV LED, charge management can be performed outside the science band. A charge management system has also been demonstrated on board the SaudiSat in a MGRS-like configuration using a single bias plate with large gap size, UV LED light source, and a single large spherical proof mass as shown in Fig. 6. For the present instrument, passive charge management will be used, relying on a virtual wire generated by photoemission and without bias, suitable for the proposed low capacitance (~2 picofarad) TM.

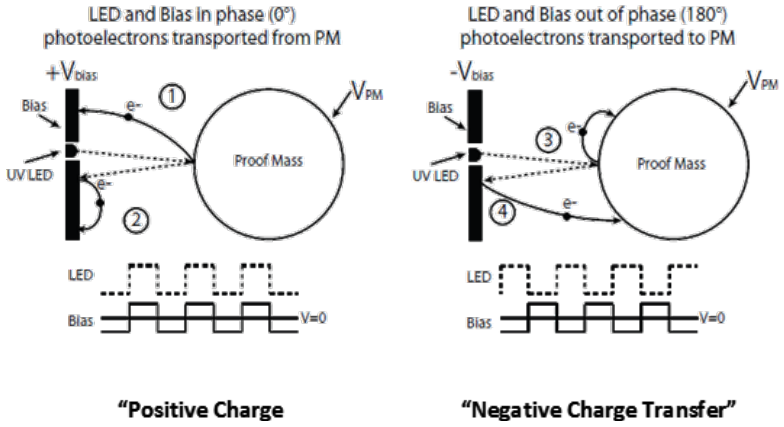

Figure 6. Charge management. Schematic showing the basic operation of charge management. The solid lines describe the electron path while the dashed lines describe the UV path. When the bias plate voltage relative to the housing (V_{bias}) is positive, (1) photoelectrons generated from the proof mass and (2) photoelectrons generated from the bias plate travel to the bias plate leading to an increase in the proof mass potential (V_{PM}). When V_{bias} is negative, (3) photoelectrons generated from the proof mass and (4) photoelectrons generated from the bias plate travel to the proof mass leading to a decrease in V_{PM}.

Fig. 7 shows a CAD model and a prototype of the TM housing with the shape memory alloy (SMA) based trigger mechanism for uncaging. The SMA is made of Nitinol, which is composed of nickel and titanium, with the balance set up for an activation temperature of 70°C.

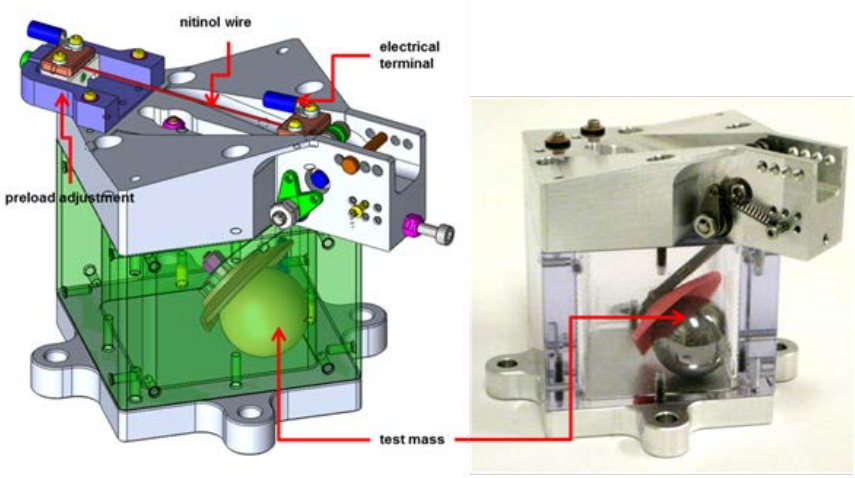

Figure 7. Caging mechanism. Model of the caging mechanism showing the use of SMA to trigger uncaging (left). Photograph of the caging system fabricated at Stanford (right).

Technology Demonstration Payload: Drag-Free Control System

The drag-free Attitude and Translation Control (ATC) system for the MGRS mission has the requirement of a residual acceleration smaller than 10^{-12} $m \cdot s^{-2} \cdot Hz^{-1/2}$ from 10 mHz to 1 Hz. ATC is a 6 degree-of-freedom (DOF) sensing and actuation system. The primary 3 DOF translation sensor is the DOSS. Attitude sensing is a fusion of the star tracker and the rate gyros included in the attitude determination payload. Both drag-free and attitude control inputs, as well as the output of both attitude and translation sensors are optimally combined via an Extended Kalman Filter (EKF), providing real-time attitude and translation estimates and covariances.

Estimates of satellite attitude and angular rate (3 DOF) provided by the EKF are fed into the attitude controller loop, which sends a command to the appropriate cold gas thrusters (VACCO MEPSI[31], nominal thrust: 53mN). These thrusters provide the commanded torque to the spacecraft, whose motion is perturbed by several disturbances including atmospheric drag, solar radiation pressure, magnetic and gravity gradient induced torques. The drag-free translation control runs at 10 Hz with a bandwidth of about 1 Hz, and keeps the satellite centered at the proof-mass (see Fig. 8). Relative displacement and velocity estimates between the satellite and the proof-mass are used within the translation controller, which sends thrust commands to the micro-propulsion system. Translational control is achieved by using a set of Radio Frequency (RF) Ion engines being developed by Astrium[32] (thrust range: 5-500μN). The separation of translational and attitude control actuation allows for simplicity in the controller synthesis and inherent robustness to failures.

Redundancy will be guaranteed by the number of thrusters, the number of DOSS beams and angular sensors. The drag-free control algorithms will be designed to be agile and adaptive to loss of redundant sensors and thrusters. The overall drag-free performance will be evaluated by a ground-based precision orbit and gravity determination facility which will evaluate un-modelled perturbations through the processing of multi-GNSS measurements and the comparison with state-of-the-art static and dynamics earth gravity models. In the next sections, we detail challenges, technical approach, and preliminary results for the translation control only, as it represents the main mission enabler.

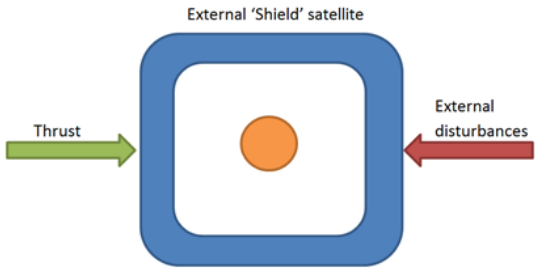

Figure 8. Drag Free Satellite. The satellite is centered at the proof-mass (orange ball at the center), shielding it from external non-gravitational forces such as aerodynamic drag and solar pressure. This allows the proof-mass to move along an almost pure gravitational trajectory.

Technology Demonstration Payload: Challenges and Technical Approach

The MGRS drag-free technology demonstration presents three key challenges. From the standpoint of residual acceleration sensitivity, the mission aims to demonstrate three-axis drag-free operations with residual non-gravitational acceleration of the proof-mass with three orders of magnitude improvement with respect to the best drag-free performance to date (achieved by Gravity Probe B[33]). From a spacecraft bus perspective, while the desired drag-free performance is comparable to the soon to be launched LISA Pathfinder mission (which aims to demonstrate single-axis drag-free operations under 10^{-14} $ms^{-2}Hz^{-1/2}$ within 1-30 mHz[34]), MGRS is a microsatellite with external dimensions of the order of 650mm. As a result, the expected external disturbances on the satellite such as aerodynamic drag and solar radiation pressure are extremely small, which requires challenging micro-thrusting capabilities. Specifically, the onboard propulsion system must be able to provide active compensation at micro-Newton levels in order to maintain a fixed distance between the proof-mass and the external satellite. Finally, the control design must be robust with respect to uncertainties of the nominal dynamics and actual disturbances.

The objective of the translation control system is to keep the satellite centered on the proof-mass. The equations of motion for the proof-mass are

$$\ddot{\vec{r}} = \vec{f}_{\text{gravity}} + \vec{f}_{\text{direct}} + \vec{f}_{\text{coupled}} \tag{1}$$

Here, $\ddot{\vec{r}}$ represents the acceleration of the proof-mass, given by the sum of the external gravitation forces (subscript gravity), direct disturbances (subscript direct), and coupled disturbances (subscript coupled) that act between the satellite and the proof-mass. The direct disturbances comprise residual non-gravitational forces not shielded by the satellite (for example, collision impacts from cosmic rays) and also include forces due to differential radiation pressure as a result of outgassing of satellite's components. Since direct disturbances are not affected by the relative position of the proof-mass with respect to the satellite, they can not be rejected via control design and therefore represent a fundamental lower bound on achievable drag-free performance. The coupled disturbances arise from electromagnetic interactions and mass-attraction forces exerted by the satellite on the proof-mass. These forces can be approximated locally about equilibrium according to a virtual spring model[35]

$$\vec{f}_{\text{coupled}} = K\left(\vec{r} - \vec{r}_{\text{eq}}\right) \tag{2}$$

where $\vec{r}_{\text{eq}}$ denotes the (unknown) position of the spring equilibrium, fixed within the central satellite cavity. Assuming a diagonal stiffness matrix, numerical experiments similar to the analysis for the LISA mission[35], provide an estimate for the diagonal components of *K* which are less than $10^{-7}\ s^{-2}$. Using this upper bound, the translational control objective can be equivalently stated as the requirement that the relative displacement between the proof-mass and the satellite is less than $10^{-7}\ mHz^{-1/2}$ within the target bandwidth, i.e., 10 mHz – 1 Hz.

The translation control scheme is critically affected by several disturbance forces and torques acting on the satellite and proof-mass. Accordingly, a high-fidelity simulation environment that models the various effects on the proof-mass and satellite has been developed, which includes[36]

- high order spherical expansion model for the gravitational field, including tidal effects,
- aerodynamic drag using high-fidelity density and atmospheric wind models (using long-term solar and geomagnetic activity predictions),
- solar radiation pressure drag due to direct and off-earth reflection (albedo),
- mutual gravitational attraction and electromagnetic coupling between spacecraft and proof-mass,
- sensing (DOSS) and actuation (thrusters) noise,
- disturbance torques associated with the various disturbance forces.

This modeling framework allows the computation of an envelope for the expected satellite disturbance profiles and the derivation of sizing constraints for a suitable micro-propulsion system, as detailed below.

Figure 9 shows the expected aerodynamic and solar radiation pressure forces on the satellite computed for a 328-km Sun-synchronous dawn-dusk orbit, assuming a spacecraft attitude aligned with the radial, in-track, and cross-track directions. The in-track and cross-track forces are large enough (max > 20 μN) to be continuously compensated through existing ion-thruster technology, namely the Astrium's μ-X RF Ion engines[32]. On the contrary, the radial forces are very small (order of ±4μN), and can only be counteracted by a dedicated attitude mode that is offset from the nominal orbital frame. The disturbances at higher altitudes (for instance at 650km) are even smaller (order of ±8μN in all axes) due to the lower atmospheric density. The lack in maturity in micro-propulsion

to provide thrust at such low levels is therefore one of the primary motivating factors for choosing a lower orbit (in addition to the gravimetric science objectives discussed earlier).

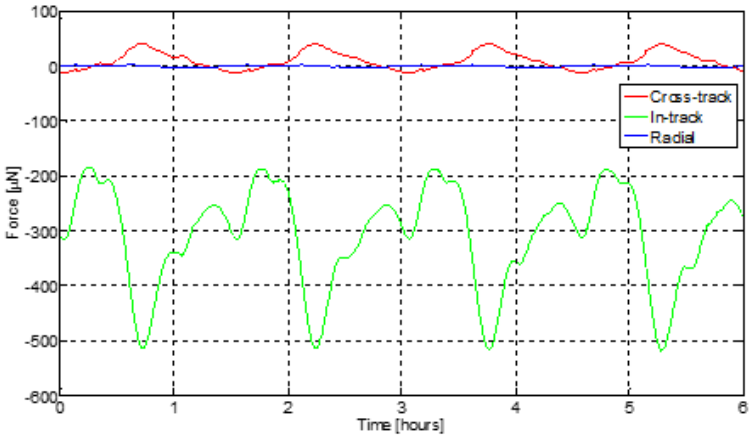

Figure 9. Expected disturbances. Aerodynamic drag and solar radiation pressure at 328 km altitude.

Using such disturbance modeling results and a detailed propulsion trade-study, a preliminary ATC that uses the Astrium's Ion engines and VACCO cold-gas micro-propulsion thrusters has been developed. The generalized translation control system architecture is shown in Fig. 10.

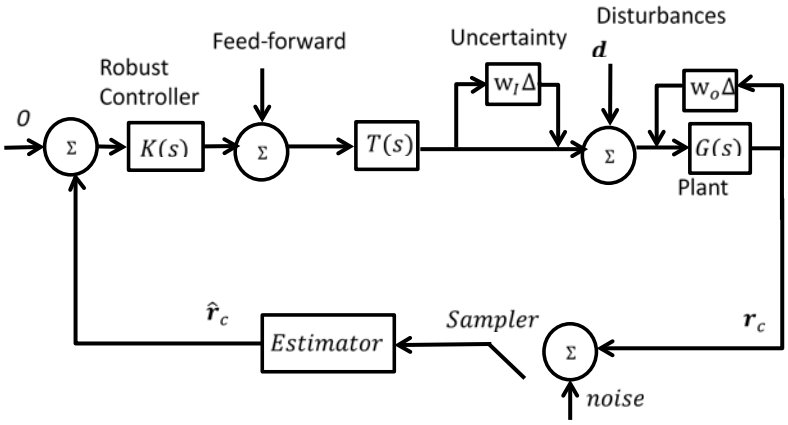

Figure 10 Translational control. Generalized translational control system architecture. $\vec{r}_c$ denotes the relative displacement between the satellite and the proof-mass.

The preliminary design approximates the Multi-Input-Multi-Output (MIMO) plant as three decoupled Single-Input-Single-Output (SISO) plants. Accordingly, three decoupled SISO controllers are designed and simulation results suggest a residual acceleration for the proof-mass under 10^{-12} $m{\cdot}s^{-2}{\cdot}Hz^{-1/2}$ in nominal conditions (no uncertainty in system dynamics). While the decoupled approximation is an over-simplification of the true MIMO dynamics, it is sufficient to gain key insights into the fundamental limitations of performance, and to provide a proof of concept.

The decoupling simplification will be relaxed in future work in favor of a more advanced design approach for MIMO systems. In particular, optimization-based robust control techniques such as H_∞ and μ-synthesis will be explored to guarantee robust performance[37, 38]. In addition, a stochastic Model-Predictive-Control (MPC) algorithm is under investigation which addresses the uncertainty and disturbance rejection problem in a less conservative fashion than robust control techniques.

THE MSTAR MISSION: KEY PAYLOAD TECHNOLOGIES

Science Payload: Motivation

The scientific objective of mSTAR is to achieve a two order of magnitude improvement in the search for Lorentz invariance violations using technologies well-developed on the ground, but performing the observations in space. The mSTAR mission will improve our understanding of the range of applicability of the theory of Special Relativity (SR), a cornerstone for understanding the laws governing the universe and its evolution. To achieve a two order of magnitude improvement on the resolution of the Kennedy-Thorndike (KT) coefficient, measurement will be performed by comparing the frequency of an optical transition in molecular iodine with the resonant frequency of a high-finesse optical cavity. Figure 11 illustrates the functioning principle and a possible direction and velocity of a preferred frame given by the cosmic background radiation.

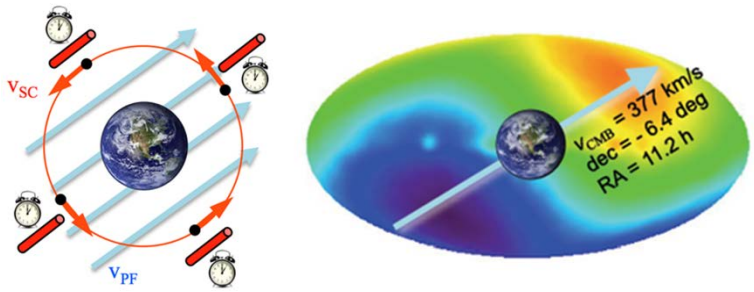

Figure 11. **mSTAR functioning principle**. Experiment concept (left) and velocity of earth relative to a possible preferred frame like the cosmic microwave background radiation.

It is well known that SR owes its experimental foundation to a minimum of three types of classical experiments: those of Michelson and Morley (MM)[39], Kennedy and Thorndike (KT)[40] and Ives and Stilwell[41]. Extreme precision has been obtained in verifying SR in many areas, yet the basis for acceptance must remain experimental, as with all laws of physics. Recently, a more detailed approach has been developed to categorize potential manifestations of Lorentz invariance violations (LIV) that might occur within all sectors of the Standard Model (SM). A generalized extension to the SM (SME) was developed and a classification scheme for possible small effects was presented. With the restriction to the photon sector of the SME and renormalizable terms, a sub-group of the coefficients of LIV was found to be related to the putative angle dependence of speed of light (c) within a Sun-centered near-inertial reference frame. This implied their detectability with MM type experiments. With the same restrictions, an analysis of KT type experiments yielded similar terms. However from a broader perspective it is now recognized that higher order terms are critical to the analysis of these latter experiments. An essential feature of a KT experiment is to study the boost-dependence of c rather than its angle dependence.

To date, efforts to place limits on LIV related to KT effects have relied on the earth's rotational and orbital motions to modulate the velocity of an apparatus relative to some inertial reference. The resulting limits on the constancy of c are on the order $\delta c/c \sim 10^{-16}$. While improvements in technology will no doubt lead to further gains, it has become clear that space experiments in LEO offer a way to obtain much better results than with ground experiments. The intrinsic boost-dependence of a KT experiment can easily be seen from the idealized model of Mansouri and Sexl (MS)[42] that separates small LIV terms into angle and boost dependent groups. Analyzed by Robertson[43] and MS, the RMS model of Lorentz violations can be parameterized as

$$\delta c/c = \varepsilon_{KT}(v/c)^2 + \varepsilon_{MM}(v/c)^2 \sin^2\theta \qquad (3)$$

where the quantities ε_{KT} and ε_{MM} are small dimensionless coefficients, θ is the angle of propagation of light relative to some preferred direction, v is the velocity of the apparatus relative to the frame, and δc is the deviation of c from an exact constant. In SR, the two terms on the right hand side are zero. In the RMS model, a MM experiment can be viewed as measuring the quantity ε_{MM} via the θ-dependence of c, while a KT experiment measures the quantity ε_{KT} via the velocity dependence of c, independent of θ. A generalized experiment may be sensitive to both terms.

Performing the experiment in space offers a number of advantages over ground experiments. In particular, with a well-designed spacecraft the vibration environment can be extremely quiet. Large gravity forces are eliminated, allowing the possibility of very soft mounting of force-sensitive components. Of course, latching during launch is necessary, but these can be retracted during science measurements. The wide range of orbits available allows much better optimization of the experimental conditions than an equivalent ground experiment. For LEO, the velocity modulation in Eq. (3) is typically 25 times larger than in a ground experiment using the earth's rotation. The correspondingly short period of the velocity reversals is another major advantage because it greatly mitigates the thermal control problem. Also, it allows a large reduction in the secular drift requirements for the rods and clocks. A dawn/dusk sun-synchronous orbit has two further advantages. The spacecraft can be in sunlight for almost the entire year minimizing thermal effects, and orbit plane precession can be used to sweep the entire sky for velocity effects. The various motions involved also allow the separation of some systematic effects from signals aligned with inertial coordinates. The distribution of $\delta c/c$ variations on the sky as seen as a function of orientation and spacecraft velocity vector at the orbital period represent the raw data obtained from the mSTAR instrument from which all other results are derived.

The goal of the experiment is to reduce the noise on the frequency comparison to below 1 part in 10^{17} of the optical frequency in a nominal 2-year LEO mission. However this level of performance has not yet been demonstrated on the ground. Therefore the mission sensitivity requirement is set at $5{\cdot}10^{-17}$ in a 2-year mission, which translates to an Allan deviation[43] of $5{\cdot}10^{-15}$ at orbital period. This level of performance has already been demonstrated on the ground and allows for immediate space hardware development. It is also required that the data from up to 10,000 orbits over the 2 years can be averaged to reach the $5{\cdot}10^{-17}$ level for the mission sensitivity requirement. Since no consumables are required for the mission, the 2-year duration is a soft lower bound.

Science Payload: Instrument

The mSTAR instrument comprises a highly stable optical cavity located in a thermal enclosure that maintains high vacuum conditions, an iodine frequency reference with very high stability and low noise, and associated electronics and software. A functional diagram of the mSTAR payload is shown in Fig. 12. It consists of the following subsystems:

- Iodine based frequency reference (clock 1) with laser source Beam Preparation Unit (including second harmonic generator and acousto-optic modulators)
- Cavity based frequency reference (clock 2) with thermal enclosure and Modulation Bench (including acousto-optic modulators and electro-optic modulator)
- Control electronics for clocks 1 and 2
- Laser control electronics
- Data Management Unit (DMU) and Power Conditioner

There are two input signals, emanating from the common source – clock 1, an absolute clock – a laser stabilized to an energy transition in molecular iodine (I_2) as shown in Fig. 13. The first signal is the baseline used to compare the signal from clock 2, the so-called rod. It goes directly from the laser clock to a frequency comparator.

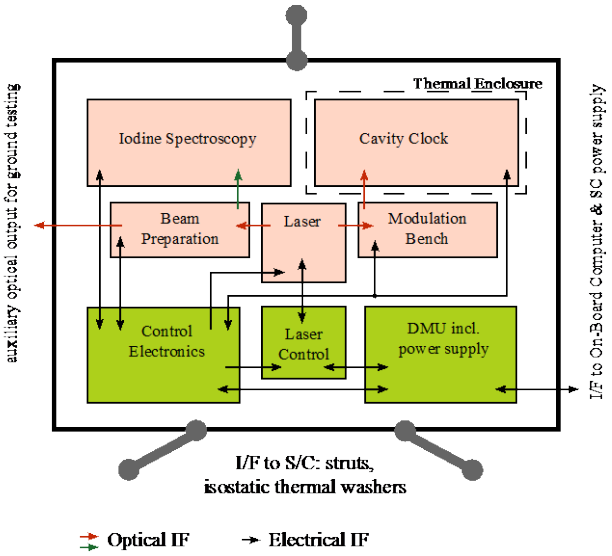

Figure 12. **mSTAR payload**. Functional diagram of the mSTAR payload.

The second signal is fed into a resonant cavity, clock 2, via a frequency shifter. The cavity and the shifter are in a feedback loop such that the frequency shifter can maintain the light frequency at the proper cavity resonance at all times. Either length contraction in the rod and/or time dilations will manifest themselves as deviations in the required frequency shift to keep the rod resonant with the laser light. The output of the rod laser light is then compared with the baseline signal to generate the KT science output. The rod is made of Ultra-Low Expansion (ULE) glass to reduce spurious thermal effects as shown in Fig. 14. The payload also includes the corresponding control electronics for the two clocks (including temperature stabilization, frequency control feedback loop) and the laser (including temperature stabilization, low-noise current drive). A data management unit controls the experiment, collects the data, and acts as interface to the on-board computer, which is assumed to be part of the spacecraft bus.

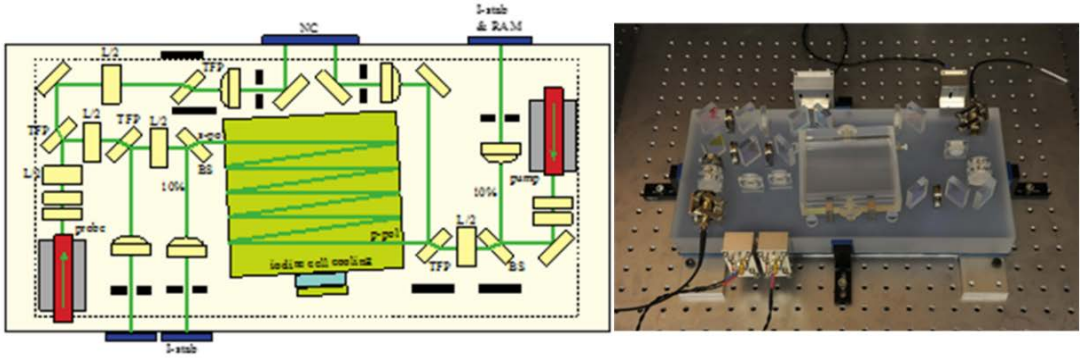

Figure 13. **mSTAR spectroscopy unit**. Schematic (left) and photograph (right) of the iodine spectroscopy unit (engineering model setup). TFP is the thin film polarizer, L/2 is the half-waveplate, BS is the beam splitter, NC is the noise cancelling detector, I-stab is the intensity stabilization, and RAM is the residual amplitude modulation.

The iodine instrument is based on modulation-transfer-spectroscopy (MTS) techniques applied to a molecular species in gas phase[44]. These techniques employ two counter-propagating laser beams (pump and probe beam) through an iodine sample for Doppler-free resolution of narrow transitions. MTS has been applied extensively to hyperfine transitions in molecular iodine using

frequency doubled Nd:YAG lasers operating at 1064 nm. Nd:YAG lasers feature a superior intrinsic frequency and intensity stability, while I_2 features strong, narrow hyperfine transitions at 532 nm. These can be addressed with a frequency-doubled portion of the fundamental output of the Nd:YAG laser. The natural linewidth of the most interrogated hyperfine transition (the a_{10} component of the R(56) 32-0 line) is 280 kHz. Taking into account transition broadening, pressure broadening and power broadening the typical linewidth is ~ 800 kHz.

Current setups have achieved a stability of $4 \cdot 10^{-15}$ at orbit time[45] meeting the requirement of the mSTAR mission. Many issues limiting the long-term performance have been identified[46-48]. Some of the major issues are residual amplitude modulation (RAM) and pointing stability of the beams in the cell. Methods for control of RAM have been developed[48]. In the setup proposed for mSTAR, the pointing instability will be significantly reduced through the use of a thermally and mechanically stable assembly-integration technology.

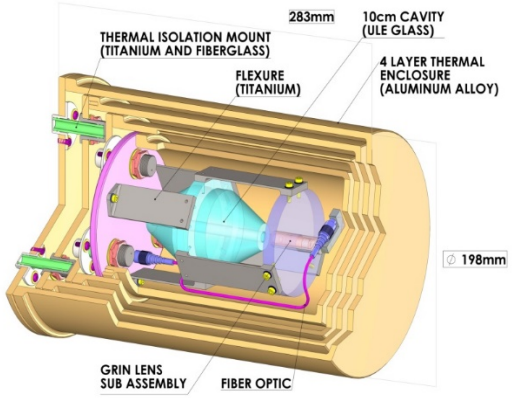

Figure 14. **mSTAR ultra-stable cavity**. Schematic of the fiber-coupled, ultra-stable ULE cavity inside a 4-layer thermal enclosure.

The effectiveness of the cavity as a frequency sensor depends strongly on the line width and stability of the laser sources, the thermal-mechanical stability of the cavity itself, and the sensitivity of the cavity to velocity-induced length perturbations. The sensitivity correlates most directly to cavity finesse which is defined as the ratio of the free spectral range of the cavity to the full width at half maximum of the cavity resonance peak. The required finesse is >100,000 to detect length perturbations at sensitivities necessary to meet the science requirement (i.e., $\Delta l/l = 10^{-15}$ at orbit period, where l is the cavity length). Modern cavities readily reach finesse values well above 100,000[49-50]. The cavity design supports the finesse requirement using pairs of low-absorption (<5 ppm), partially transmitting (T< 20 ppm) mirrors (achievable finesse > 160,000).

High elastic moduli and the thermal behavior of ULE glass drive the material selection for the cavity body. ULE has a low coefficient of thermal expansion (CTE) of ~10^{-9}/K within an operating temperature range of 10 – 30 °C, and a null CTE near 15 °C[51]. Higher null temperatures are available on special order. In conjunction with thermal enclosure providing temperature stability between 0.1 – 1 μK, the mechanical stability of ULE is adequate to meet the 10^{-15} length stability at orbit period required to achieve the science objective.

For the KT measurement the signal from the reference clock is initially compared to the signal from the rod via the frequency comparator while the apparatus is in an initial velocity state. There will be some difference in the two frequencies that is recorded. Later, when the apparatus is travelling in the opposite direction around the orbit relative to its initial state, the signals are compared again. If there is no difference from the recorded value, the KT portion of the experiment is null. If

there is a difference from the recorded value, the KT coefficients may be precisely determined by the difference between the initial vs. boosted frequency values. The frequency comparison is made with opposing velocities in three orthogonal directions.

Technology Demonstration Payload

The technology demonstration payload on-board mSTAR seeks to demonstrate the capability to perform rendezvous, including approach and receding maneuvers, with respect to a non-cooperative passive Space Resident Object (SRO) using vision-based angles-only navigation. In addition to the research and development roadmap described in this paper (see Fig. 1-3), the proposed experiment serves the needs of a new class of on-orbit servicing missions which is under investigation by several national and international space agencies[52-53]. As a matter of fact, the capability to approach and rendezvous with a non-cooperative SRO in a safe, fuel efficient, and accurate manner is a fundamental requirement of future satellite missions for debris removal, inspection and repair, and sample return (Mars, Titan, etc.).

The proposed payload builds on the experience gained from the PRISMA mission[7] where the author demonstrated a ground-in-the-loop rendezvous in the range of 30-3 km with a passive target based on angles-only navigation during the so-called Advanced Rendezvous Experiment using GPS and Optical Navigation (ARGON)[54]. Since the SRO employed in the mSTAR mission is a 1U CubeSat deployed by the mothership satellite itself, the focus of the experiment is on far- to mid-range separations from about 10 km to hundreds of meters in the along-track direction. The experiment will take place at the beginning or end of the mSTAR mission and lasts one month.

The use of angles-only navigation is appealing because it relies on simple passive low-cost sensors (e.g., optical or infrared cameras) able to provide the line-of-sight (LOS) direction to the target object. To this end, star trackers usually employed for attitude determination can be advantageously used to track a SRO, if properly oriented[55]. At sufficiently large separations, it is acceptable to approximate the center of mass of the client satellite with its intensity centroid and angles-only navigation represents a sufficiently accurate methodology to accomplish the first phases of the approach. This leads to simpler and cheaper designs of the servicer satellite, limiting the use of more complex sensors (e.g., radar, lidar, stereo-cameras) to close-proximity operations. From a performance point of view, the mSTAR technology demonstration aims at unprecedented relative navigation accuracies to within 10 m (standard deviation) for all relative orbit elements, except for the relative mean argument of latitude (i.e., mean along-track separation) which is estimated with errors within 10% of the inter-spacecraft separation due its weak observability.

As compared with previous flight experiments, the main contribution of mSTAR will be to accomplish the vision-based navigation and control tasks in a fully autonomous manner on-board the mothership spacecraft. In this scenario, key challenges are given by the limited computational resources, the high level of robustness required to cope with system and environment uncertainties, and the specific constraints posed by the satellite bus and mission operations. The challenges will be tackled by novel guidance, navigation and control algorithms tailored to the angles-only rendezvous problem under development at Stanford. These leverage advanced space mechanics (especially Gauss Variational Equations in combination with relative orbit elements theory)[56], non-linear estimation theory (especially unscented Kalman filtering in combination with consider covariance theory)[57], and stochastic MPC approaches[58] aided by closed form solutions to reduce the computation effort.

The most promising sensors and actuators identified for the technology demonstration are 1) the Nano Star Tracker by Blue Canyon Technologies[57] for image generation, which employs a high resolution CMOS sensor immune to blooming effects plaguing older CCD sensors, 2) the GNSS

Javad Triumph DG3TH and the NovAtel OEM4-G2L receivers[19] for real-time absolute orbit and maneuver estimation of the servicer spacecraft, and the 3) VACCO cold-gas micro-propulsion thrusters[31] for impulsive maneuvering.

CONCLUSION

This paper has described a 10-year research and development roadmap under implementation at the KACST-Stanford's Center for Excellence in Aeronautics and Astronautics in collaboration with national and international partners. The ultimate goals are to 1) develop a multi-purpose reconfigurable precise distributed space system (DSS) based on microsatellite platforms, and 2) demonstrate its unprecedented capabilities in areas such as earth gravimetry and system dynamics, gravitational waves detection, and on-orbit servicing. After an overview of the schedule and the identified enabling technologies, the first milestones of the program have been presented in details with a focus on the science and technology payloads. In particular the Modular Gravity Reference Sensor (MGRS) mission, currently planned for 2019, will demonstrate drag-free technologies with aimed residual acceleration noise below 10^{-12} m/s^2. The primary science objective of MGRS is the determination of the static earth gravity field with improvement of up to two orders of magnitude in accuracy as compared with ground-based observations. Lessons learned from MGRS and dedicated laboratory demonstrations will precede the launch of the Miniaturized Space Time Asymmetry Research on a Small Satellite (mSTAR) in 2021. This mission has two fundamental technology objectives, namely 1) the demonstration of unprecedented timekeeping capabilities using molecular iodine clocks, and optical cavity resonators, and 2) the demonstration of vision-based far- to mid-range rendezvous relative to a non-cooperative CubeSat carried and ejected on-orbit by the mother spacecraft. The science objective of mSTAR is an advanced Kennedy-Thorndike test of special relativity using the large and rapid velocity modulation available in low earth orbit. An improvement of about two order of magnitudes over present ground results are expected. The successful execution of advanced missions such as MGRS and mSTAR will mature the fundamental navigation, control, timekeeping, and drag-free technologies needed to realize a multi-purpose DSS. At the same time, breakthroughs in gravitational physics and on-orbit servicing will push the boundaries of space science and exploration.

REFERENCES

[1] J. Leitner, "Distributed Space Systems: Mission Concepts, Systems Engineering, and Technology Development," Systems Engineering Seminar, April 2, 2002, NASA-GSFC at http://ses.gsfc.nasa.gov/ses_data_2002/020402_Leitner_DSS.pdf, Last accessed on May 2015.

[2] K.T. Alfriend, S.R. Vadali, P. Gurfil, J.P. How, L.S. Breger, "*Spacecraft Formation Flying: dynamics, control, and navigation*." Elsevier Astrodynamics Series, 1st ed., 2010.

[3] D.C. Woffinden and D.K. Geller, "*Navigating the Road to Autonomous Orbital Rendezvous*," Journal of Spacecraft and Rockets, Vol. 44, No. 4 (2007), pp. 898-909. DOI: 10.2514/1.30734

[4] T. Kasai, M. Oda, and T. Suzuki, "*Results of the ETS-7 Mission - Rendezvous Docking and Space Robotics Experiments*," Proceedings of the Fifth International Symposium on Artificial Intelligence, Robotics and Automation in Space, ISAIRAS '99, 1-3 June, 1999, ESTEC, Noordwijk, the Netherlands. Edited by M. Perry. ESA SP-440. Paris: European Space Agency, 1999, p.299

[5] Airforce Research Laboratory (AFRL), Space Vehicles Directorate, "*Fact Sheet on XSS-11 microsatellite*," Current as December 2005, http://www.kirtland.af.mil/shared/media/document/AFD-070404-108.pdf, Last accessed on May 2015.

[6] T.A. Mulder, "*Orbital Express Autonomous Rendezvous and Capture Flight Operations*," AIAA/AAS Astrodynamics Specialist Conference and Exhibit, AIAA 2008-6768, 18-21 August 2008, Honolulu, Hawai.

[7] S. D'Amico, P. Bodin, M. Delpech, R. Noteborn, "*PRISMA*," Chap 21, pp. 599-637. In: D'Errico M. (Ed.) Distributed Space Missions for Earth System Monitoring Space Technology Library, 2013, Volume 31, Part 4. DOI 10.1007/978-1-4614-4541-8_21

[8] G. Krieger, et al., "*TanDEM-X*," Chap 13, pp. 387-435. In: D'Errico M. (Ed.) Distributed Space Missions for Earth System Monitoring Space Technology Library, 2013, Volume 31, Part 4. DOI 10.1007/978-1-4614-4541-8_21

[9] M.D. Graziano, "*Overview of Distributed Missions*," Chap 12, pp. 375-386. In: D'Errico M. (Ed.) Distributed Space Missions for Earth System Monitoring Space Technology Library, 2013, Volume 31, Part 4. DOI 10.1007/978-1-4614-4541-8_21

[10] J.F. Flury, R. Rummel, "*Future Satellite Gravimetry and Earth Dynamics*," Springer, 2015, ISBN 0-387-29796-0

[11] G.K. Skinner, B.R. Dennis, J.F. Krizmanic, and E.P. Kontar, "*Science Enabled by High Precision Inertial Formation Flying*," pp. 599-637. In: S. D'Amico and Z.H. Zhu (Ed.), Special Issue on Spacecraft Formation Flying – Part I, Int. J. Space Science and Engineering, Vol. 1, No. 4, 2013.

[12] W. Cash, J. Kasdin, S. Seager, and J. Arenberg, "*Direct Studies of Exo-planets with the New Worlds Observer*," Proc. SPIE 5899, UV/Optical/IR Space Telescopes: Innovative Technologies and Concepts II, 58990S, 31 August 2005. DOI: 10.1117/12.617377

[13] Proceedings of the 7th International LISA Symposium, 16–20 June 2008, Barcelona, Spain. In: Journal of Physics: Conference Series, Volume 154, 20 April 2009.

[14] M. O'Neill, H. Yue, S. Nag, P. Grogan, O. de Weck, "Comparing and Optimizing the DARPA System F6 Program Value-Centric Design Methodologies," AIAA SPACE 2010 Conference & Exposition, AIAA 2010-8828, 30 August-2 September 2010, Anaheim California

[15] KACST news, Riyadh, Saudi Arabia, 20 June 2014, "*KACST launched its thirteenth Satellite (Saudisat-4)*", http://www.kacst.edu.sa/ en/about/media/news/Pages/news658.aspx

[16] G. Balmino, R. Rummel, P. Visser, P. Woodworth, J. Johannessen, and M. Aguirre, "*Gravity Field and Steady-State Ocean Circulation Explorer, Reports for Mission Selection, The Four Candidate Earth Explorer Core Missions*," SP-1233 (1), 217 pp., July 1999

[17] S. D'Amico, Ch. Arbinger, M. Kirschner, S. Campagnola, "*Generation of an Optimum Target Trajectory for the TerraSAR-X Repeat Observation Satellite*," 18th International Symposium on Space Flight Dynamics, 11-15 Oct. 2004, Munich, Germany.

[18] O. Montenbruck, P. Ramos-Bosch, "Precision Real-Time Navigation of LEO Satellites using Global Positioning System Measurements. GPS Solutions 12(3):187–198. doi:10.1007/s10291-007-0080-x

[19] O. Montenbruck, S. D'Amico, "GPS Based Relative Navigation," Chap 5, pp. 185-223. In: D'Errico M. (Ed.) Distributed Space Missions for Earth System Monitoring Space Technology Library, 2013, Volume 31, Part 4. DOI 10.1007/978-1-4614-4541-8_21

[20] D. B. DeBra, "*Disturbance compensation system design*," APL Technical Digest, 12, 14 (1973); Staff of the Space Department, The Johns Hopkins University Applied Physics Laboratory, Silver Spring, MD and Staff of the Guidance and Control Laboratory, Stanford University, Stanford, CA. *A satellite freed of all but gravitational forces: "TRIAD I"*, American Inst. of Aero. & Astro. Journal (AIAA), 11, 637 (1974).

[21] C. W. F. Everitt, et al, "*Gravity Probe B: Final Results of a Space Experiment to Test General Relativity*," Physical Review Letters, Volume 106, 221101, (2011).

[22] Canuto, "*Drag-free Attitude Control for the GOCE Satellite*," Automatica, Volume 44, 1766 (2008).

[23] S. Buchman, J. P. Turneaure, "*The Effects of Patch-Potentials on the Gravity Probe B Gyroscopes,"* Rev. Sci. Instrumentation, **82**, 074502 (2011).

[24] K. Sun, G. Allen, S. Buchman, R. L. Byer, J. W. Conklin, D. B. DeBra, D. Gill, A. Goh, S. Higuchi, P. Lu, N. A. Robertson, and A. J. Swank, "*Progress in Developing the Modular Gravitational Reference Sensor*," Laser Interferometer Space Antenna, 6th International LISA Symposium, AIP Conference Series, Volume 873, 515 (2006).

[25] A. Zoellner, E. Hultgren, and K. Sun, "*Integrated Differential Optical Shadow Sensor for Modular Gravitational Reference Sensor*," http://arxiv.org/abs/1302.1623, and A. Zoellner et al., *Differential Optical Shadow Sensor CubeSat Mission*, Proc. AIAA/USU Conference on Small Satellites, Advanced Technologies II, SSC12-IX-6 (2012).

[26] K. Balakrishnan, et al, "*UV LED Charge Control of an Electrically Isolated Proof Mass in a Gravitational Reference Sensor Configuration at 255 nm*," submitted to Classical and Quantum Gravity, Preprint: arxiv.org/abs/1202.0585.

[27] A. Zoellner, E. Hultgren, and K. Ingold, "*Final Report: Caging System for Drag-free Satellites*," https://spacegrav.stanford.edu (2013).

[28] J. C. Cooley, M. C. Aronson, "*Origins of Paramagnetism in Beryllium-Copper Alloys*," J. Alloys and Compounds, Volume 228, 195 (1995).

[29] J. C. Mester, J. M. Lockhart, "*Remanent Magnetization of Instrument Materials for Low Magnetic Field Applications*," Czech. J. Phys, Volume 46 (1996) Suppl. S5.

[30] S. Saraf, K. Balakrishnan, S. Buchman, R. Byer, D. Faied, J. Hanson, B. Jaroux, C. Y. Lui, and M. Soulage, "*UV LED Charge Control of an Electrically Isolated Proof Mass in a Gravitational Reference Sensor Configuration at 255nm*, in *Latin America Optics and Photonics Conference*, OSA Technical Digest (online) (Optical Society of America, 2014), LM2A.4.

[31] VACCO, Data Sheet, http://www.vacco.com/images/uploads/pdfs/MicroPropulsionSystems_0714.pdf,. Last accessed on May 2015.

[32] H. J. Leiter, C. Altmann, D. Lauer, and R. Kukies. "*Miniaturized radio frequency ion thrusters and systems – technology development and applications.*" In Propulsion and Energy Forum, pages –. American Institute of Aeronautics and Astronautics, July 2014

[33] J. Mester and S. Buchman. "*Precision Attitude and Translation Control Design and Optimization.*" In astro2010: The Astronomy and Astrophysics Decadal Survey, vol. 2010, p. 41. 2009.

[34] W. Fichter, P. Gath, S. Vitale, and D. Bortoluzzi, "*LISA Pathfinder drag-free control and system implications*." Classical and Quantum Gravity 22, no. 10 (2005): S139.

[35] D. Gerardi, G. Allen, J. W. Conklin, K-X. Sun, D. DeBra, S. Buchman, P. Gath, W. Fichter, R. L. Byer, and U. Johann. Invited article: "*Advanced drag-free concepts for future space-based interferometers: acceleration noise performance*." Review of Scientific Instruments, 85(1), 2014

[36] S. Singh, S. D'Amico, M. Pavone M, "*High-Fidelity Modeling and Control System Synthesis for the MGRS Drag-Free Satellite*," 25th International Symposium on Space Flight Dynamics ISSFD, Munich, Germany, October 19 - 23, 2015. Submitted

[37] K. Zhou, J. C. Doyle, and K. Glover. "*Robust and Optimal Control.*" Vol. 40. New Jersey: Prentice hall, 1996.

[38] L. Pettazzi, A. Lanzon, S. Theil, A. F. Finzi, "*Design of Robust Drag-Free Controllers with Given Structure.*" Journal of Guidance, Control, and Dynamics, Volume 32, Number 5 (2009): 1609-1621.

[39] A.A. Michelson, E.H. Morley, "*On the Relative Motion of the Earth and the Luminiferous Ether*," Am. J. Sci., Volume 34, 333 (1887).

[40] R.J. Kennedy, E.M. Thorndike, "*Experimental Establishment of the Relativity of Time*," Phys. Rev., Volume 42, 400 (1932).

[41] H. E. Ives, G. R. Stilwell, "*An Experimental Study of the Rate of a Moving Atomic Clock,*" J. Opt. Soc. Am. Volume 28, 215 (1938); Volume 31, 369 (1941).

[42] R. Mansouri, R. U. Sexl, "*A Test Theory of Special Relativity*," Gen. Rel. and Grav., Volume 8, 497 (1977); ibid, p. 515; ibid, p. 809.

[43] H. P. Robertson,"*Postulate Versus Observation in the Special Theory of Relativity,*" Rev. Mod. Phys., Volume 21, 378 (1949).

[44] J. Shirley,"*Modulation Transfer Processes in Optical Heterodyne Saturation Spectroscopy*," Optics Letters, Volume 7, Number 11, 537–539 (1982).

[45] T. Schuldt, K. Döringshoff, J. Stühler, E. Kovalchuk, M. Franz, M. Gohlke, D. Weise, U. Johann, A. Peters and C. Braxmaier, "*A Compact High-Performance Frequency Reference for Space Applications*," Proc. 29th Int. Symp. on Space Technology and Science (ISTS 2013, Nagoya, Japan).

[46] J. Ye, L. Robertsson, S. Picard, L. Ma and J. Hall,"*Absolute Frequency Atlas of Molecular I_2 Lines at 532 nm*," IEEE Transactions on Instrumentation, Volume 48, Number 2, 544 (1999).

[47] K. Nyholm, M. Merimaa, T. Ahola, and A. Lassila,"*Frequency Stabilization of a Diode-Pumped Nd:Yag Laser at 532 nm to Iodine by Using Third-Harmonic Technique*," Instrumentation, Volume 52, Number 2, 284 (2003).

[48] E. Zang, J. Cao, Y. Li, C. Li, Y. Deng, C. Gao et al,"*Realization of Four-Pass I_2 Absorption Cell in 532-nm Optical Frequency Standard*," IEEE Transactions on Instrumentation and Measurement, Volume 56, Number 2, 673 (2007).

[49] A. D. Ludlow, X. Huang, M. Notcutt, T. Zanon-Willette, S. M. Foreman, M. M. Boyd, S. Blatt, and J. Ye,"*Compact, Thermal-Noise-Limited Optical Cavity for Diode Laser Stabilization at $1x10^{-15}$*," Opt. Lett., Volume 32, 641 (2007).

[50] Y. Y. Jiang, A. D. Ludlow, N. D. Lemke, R. W. Fox, J. A. Sherman, L.-S. Ma, and C. W. Oates,"*Making Optical Atomic Clocks More Stable with 10^{-16}-Level Laser Stabilization,*" Nature Photonics, Volume 5, 158-161 (2011).

[51] Corning Advanced Optics, *ULE® Corning Code 7972 Ultra Low Expansion Glass*, Corning Incorporated, www.corning.com/ule (2006).

[52] Weismuller, T., Leinz, M., "*GN&C Technology Demonstrated by the Orbital Express Autonomous Rendezvous and Capture Sensor System*," American Astronautical Society Paper 06-016, 2006.

[53] T. Rupp, T. Boge, R. Kiehling, and F. Sellmaier, "*Flight Dynamics Challenges of the German On-Orbit Servicing Mission DEOS*," 21st International Symposium on Space Flight Dynamics (ISSFD), French Space Agency, Toulouse, France, 2009.

[54] S. D'Amico, J.S. Ardaens, G. Gaias, H. Benninghoff, B. Schlepp, J.L. Joergensen, "*Noncooperative Rendezvous using Angles-only Optical Navigation: System Design and Flight Results*," Journal of Guidance, Control, and Dynamics, Volume 36, Number 6, 1576-1595, 2013. DOI 10.2514/1.59236

[55] J. L. Jørgensen, T. Denver, and P. S. Jørgensen, "*Using an Autonomous Star Tracker as Formation Flying Sensor*," 4th Symposium on Small Satellites Systems and Services, European Space Agency, La Rochelle, France, 2004.

[56] S. D'Amico, O. Montenbruck, "*Proximity Operations of Formation Flying Spacecraft Using an Eccentricity/Inclination Vector Separation*," Journal of Guidance, Control, and Dynamics, Vol. 29, No. 3, 2006, pp. 554–563. DOI:10.2514/1.15114

[57] J. Hinks, M. Psiaki,"*A Multipurpose Consider Covariance Analysis for Square-Root Information Filters*," AIAA Guidance, Navigation, and Control Conference, AIAA 2012-4599, 13-16 August 2012, Minneapolis, Minnesota.

[58] R. Larsson, S. Berge, P. Bodin, U. Jonsson, "*Fuel Efficient Relative Orbit Control Strategies for Formation Flying and Rendezvous within PRISMA,*" 29th Annual AAS Guidance and Control Conference, AAS 06-025, 4-8 February 2006, Breckenridge, Colorado.